ACS Macro Letters

Letter

pubs.acs.org/macroletters

σ Phase Formed in Conformationally Asymmetric AB-Type Block Copolymers

Nan Xie,[†] Weihua Li,*[,†] Feng Qiu,[†] and An-Chang Shi[‡]

[†]State Key Laboratory of Molecular Engineering of Polymers, Department of Macromolecular Science, Fudan University, Shanghai 200433, China

[‡]Department of Physics and Astronomy, McMaster University, Hamilton, Ontario, Canada L8S 4M1

Supporting Information

ABSTRACT: The stability of various spherical phases formed in conformationally asymmetric AB diblock and architecture asymmetric AB_m miktoarm block copolymers is investigated using self-consistent field theory. Both the conformational and architecture asymmetries are unified into a parameter of conformationally asymmetric degree, ε. We find that a complex spherical phase, the σ phase, becomes stable and its phase region expands between bcc and hexagonal phases as increasing ε. Only for large conformational asymmetry, for example, $\varepsilon = 9$ (or $m = 3$), the A15 phase becomes stable in the region between the σ phase and the hexagonal phase and its phase region terminates at the intermediate segregation region. Compared with the σ phase, the A15 phase has more favorable interfacial energy by enabling the formation of larger spherical domains, and therefore, it becomes more stable in the region of more symmetric volume fraction and stronger segregation.

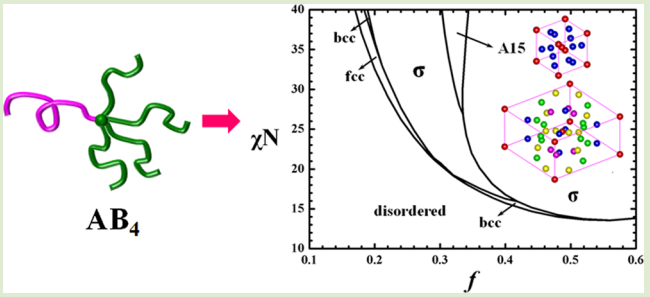

Spherical phases with tunable steric interactions formed in amphiphilic macromolecules, which provide an ideal model to study the packing of soft spheres on various crystal lattices, have attracted abiding interest.[1−14] For the packing problem of spheres, there are two well-known model examples. One is the packing of hard spheres, which is completely dominated by the entropic effect and, thus, adopts the crystalline phases of hexagonal close packing (hcp). The other is the Kelvin problem that what space-filling arrangement of equal-sized bubbles has minimal surface area, which is a pure interfacial issue. Kelvin originally proposed that the solution was the bcc lattice with the Wigner-Seitz cell of an orthic tetrakaidecahedron constructed from six square faces and eight hexagons.[15,16] After more than 100 years, Weaire and Phelan disproved this conjecture with the A15 lattice which contains two types of Wigner-Seitz cells.[16] In contrast to the above limit cases, the packing lattice of these *soft* macromolecular spheres (micelles in solution or spherical domains in melts) is not unique and is determined by two competitive roles of the entropic and enthalpic effects. For example, the packing of micelles can be modulated among fcc,[4] bcc,[5] and A15 phases[6−8] by varying the relative size between the compacting cores and the brushlike coronas, and the packing mechanism has been interpreted using an analytic argument of steric interactions by Ziherl et al.[10]

The packing mechanism of spherical domains formed in block copolymer melts is slightly different from that of the micelles formed by amphiphilic macromolecules in solution because the incompressibility of the melt enforces *micelles* to deform toward the shape of the Wigner-Seitz (or Voronoi) cells of the corresponding lattices and it is determined by the delicate balance between the entropic (stretching) energy and the interfacial energy. It has been commonly accepted that the region of spherical phases in the simplest AB diblock copolymers is mainly occupied by the bcc phase, except for a narrow hcp region near the boundary of order−disorder transition (ODT) as the phase diagram, which is governed by two thermodynamics parameters of block ratio f and the product χN of the Flory−Huggins interaction parameter χ and the total polymerization degree N, was built up by the interplay between experiment and theory in a few decades.[17−22] In 1980, Leibler constructed a phase diagram composed of the stable ordered phases of bcc sphere, hexagonal cylinder, and lamella, using a weak-segregation method.[23] Then, Matsen and Schick[20] calculated a relative complete phase diagram by developing a high-accuracy solution method of the self-consistent field theory (SCFT): the spectral method, where the novel bicontinuous phase, gyroid, was distinguished from the other bicontinuous phase, double-diamond; however, the close-packed (cp) phase was not considered and was included in a subsequent work.[24,25] For the cp phase, accurate SCFT calculations predict that the hcp lattice (*abab*··· stacking) is slightly favored over fcc (*abcabc*··· stacking) with a tiny free-energy difference.[25] Motivated by experimental observation of the *Fddd* network phase in ABC triblock copolymers,[26] Tyler

Received: July 25, 2014
Accepted: August 29, 2014
Published: September 2, 2014

and Morse explored the stability of this exotic phase not only in ABC terpolymers, but also in the simple AB diblock copolymers, which amends the phase diagram of AB diblock copolymer further.[27]

In recent experiments, Lee et al. discovered a complex spherical phase, the σ phase which contains 30 spherical domains in each unit cell, in the linear poly(1,4-isoprene-*b*-DL-lactide) (IL) diblock copolymer, as well as in the poly(styrene-*b*-isoprene-*b*-styrene-*b*-ethylene oxide) (SISO) tetrablock copolymers.[28] Driven by the reason that the σ phase is the approximate crystal structure to certain dodecagonal quasicrystals, they identified a dodecagonal quasicrystalline morphology in a subsequent work.[29] In fact, the σ phase has been identified earlier in an amphiphilic dendritic compound at a higher temperature than that at which the A15 phase was observed.[1,2] In this letter, we present SCFT calculations for conformationally asymmetric AB diblock copolymers and AB_m miktoarm block copolymers to study the relative stability of four spherical phases including fcc, bcc, A15, and the complex σ phase shown in Figure 1.

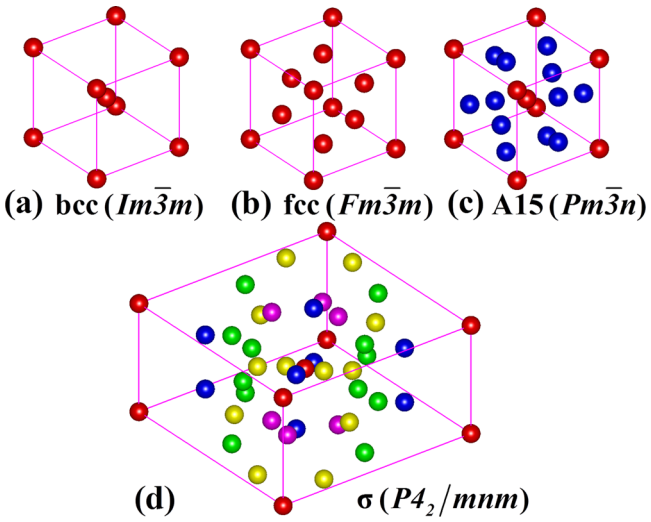

Figure 1. Schematic plots of considered spherical phases. In the unit cell of each phase, spherical domains with different Voronoi cells are plotted in different colors.

The phase diagram of AB diblock copolymers with various asymmetric conformations, which are characterized by the segment properties including segment length b_K and density ρ_K (K = A or B), has been calculated using SCFT by Matsen.[25,30] Except that the phase diagram of f and χN becomes asymmetric, no new phase is explored compared with that of the conformationally symmetric AB diblock copolymer. Indeed, the addition of branches in AB_m copolymers is another way to change the conformational asymmetry. Both factors can be unified into a conformational parameter, $\varepsilon^2 = m^2(\rho_A b_A^2/\rho_B b_B^2)$.[31] A simple argument based on the minimization of the total stretching energy suggests that a higher curvature of A/B interfaces, inside which A blocks are located, is favored by a larger value of ε for a given composition.[31−33] In other words, larger spherical domains can be formed instead of cylinders with a larger f by varying segment sizes, branching B blocks, or even superbranching. As the size of spheres increases, the shape of A/B interface is more and more influenced by the shape of Voronoi cell, that is, the polyhedral shape. The polyhedral interface favors a uniform stretching and thus optimizes the stretching energy, however, it increases the interfacial energy. The strong competition enforces the sphere packing to be changed. Grason et al. considered the third spherical phase besides the classical fcc and bcc phases, that is, A15, and identified the relative stability of spherical phases in AB_m copolymers.[34] Using a purely geometric argument, they suggested that the order of interfacial energy from low to high is A15, bcc, and fcc, whereas bcc has the most favorable stretching energy. Combining the two factors, the phase order in free energy is A15, bcc, and fcc. Then they calculated the phase diagrams of branched and superbranched copolymers using SCFT and found that the stable phase sequence of spheres is fcc, bcc, and A15, as f increases.[35,36] Besides that the branching architecture leads to the formation of a new spherical phase, it can also help to stabilize another nonspherical phase which is only metastable in the simple AB diblock and ABA triblock copolymers, e.g. perforated lamellae (PL). Very recently, Matsen systematically studied the phase diagrams of a number of AB-type copolymers with various architectures, including ABAB··· multiblock, $(AB)_n$ star, AB_n star, and comb topologies, using the spectral method of SCFT.[37] He found that the PL phase becomes stable in the phase diagrams of the AB_2 and comb copolymers, and the region of the *Fddd* phase is expanded in the two types of block copolymers.[37]

From the view of Voronoi cells, the σ phase with five different Voronoi cells of irregular polyhedra is comparable with the A15 phase with two types of polyhedral Voronoi cells because the faces of all polyhedra in the two phases are major pentagons and minor hexagons, and the weighted average numbers of faces, 13.467 and 13.5 for the σ and A15 phases, are very close. This common feature indicates that the σ phase could be a stable phase competing with the A15 phase at the phase region of large f. In addition, the σ phase has been observed in the amphiphilic dendritic compounds by experiments,[1,2] and in particular, it has also been identified in block copolymers.[28,40] To our best knowledge, however, the σ phase has not been considered as a candidate spherical phase in theory. Therefore, it is worth to reexamine the phase behaviors of sphere formation in conformationally asymmetric AB-type copolymers using SCFT calculations.

Obviously, it is a big challenge for SCFT calculations because of the large and complex tetragonal unit cell of the σ phase, which consists of 30 spherical domains. In our previous work, we proposed a valid initialization approach for the density fields in the pseudospectral method of SCFT to yield the solutions of various crystal phases formed in ABC multiblock terpolymers.[14] This initialization approach can be readily implemented to achieve the SCFT solution of the complex σ phase. The calculation details are provided in the Supporting Information (SI).

In order to determine the stability of the σ phase more quantitatively, we first reexamine the phase behaviors of spheres in the conformationally asymmetric AB diblock copolymers using the pseudospectral method of SCFT,[38,39] which have been studied by Matsen.[30] For the convenience of direct comparisons, we recalculate the phase diagrams for the same parameters, ε = 1.5 and 2.0, respectively, in Figure 2. As there is no new result about the nonsphere phases, we do not present their phase boundaries. Notice that we consider the fcc phase with a cubic unit cell instead of the hcp phase in this letter. Indeed, we verified that the fcc phase has slightly higher free energy than the hcp phase in our block copolymers, however the phase boundaries are influenced in a limited degree because

dx.doi.org/10.1021/mz500445v | ACS Macro Lett. 2014, 3, 906−910

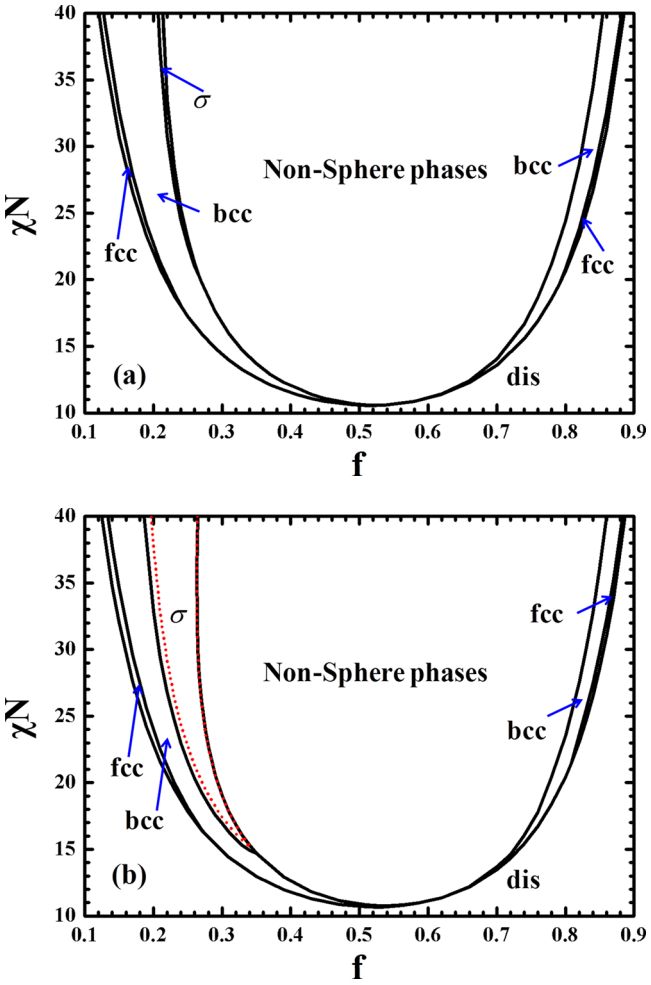

Figure 2. Phase diagrams of conformationally asymmetric AB diblock copolymers with (a) $\varepsilon = 1.5$ and (b) $\varepsilon = 2.0$. The portion of nonsphere phases is not shown. (b) The boundaries between the metastable phase A15 and the bcc and the hexagonal phases are plotted in red dashed lines.

the free-energy difference per chain is about in the order of $10^{-5}k_BT$. In the left side of the phase diagram with $\varepsilon = 1.5$, the σ phase as a stable phase appears in a very narrow region between the bcc and hexagonal phases, and its phase region ends at the triple point of (0.266, 20.322). When ε is increased to be 2.0, the region of the σ phase is significantly expanded toward both directions of increasing and decreasing f.

In the experiments by Lee et al., the σ phase was discovered by annealing the PI-*b*-PLA diblock copolymer melts of $f_{PLA} \approx 0.22$ at 25 °C lower than the temperature 40 °C at which the bcc phase was achieved (the ODT is around 50 °C).[28,40] Clearly, the phase sequence from disorder, to bcc, and then to the σ phase in our phase diagrams is consistent with the experimental observations. The conformational asymmetry as one of the critical factors was attributed to the formation of the σ phase instead of bcc, and the segment length ratio was estimated as $b_{PLA}/b_{PI} \approx 1.2$ at 140 °C.[40] Although the conformational asymmetry purely induced by the segment length ratio is still smaller than the critical value of 1.5 for stabilizing the σ phase, there are other uncertain factors influencing the conformational asymmetry, for example, the temperature and the segment densities. If we assume that the conformational asymmetry in the experimental sample is close to $\varepsilon = 2.0$, the ODT is $\chi N_{ODT} \approx 20.5$, and the phase transition between the bcc and σ phases is $\chi N \approx 26.7$ in Figure 2b. The two transition points are rather close to those estimated by Lee et al.[28,40]

As discussed above, the architecture asymmetry can be unified into the conformational asymmetry for considering the impact on the phase behaviors of AB-type block copolymers. The phase diagrams of AB_m miktoarm block copolymers, with $m = 2$, 3, and 4, are determined in Figure 3. In all three phase diagrams, the σ phase occupies a major spherical phase region, and its expansion compresses the bcc region more and more as m increases. For $m = 3$ and 4, the stability region of the A15 phase becomes noticeable between the σ and cylinder phases, and it expands mainly toward the direction of increasing f as m increases. The triple point of the cylinder, A15 and σ phases is at (0.322, 29.972) for $m = 3$, and it moves toward larger f and lower χN, (0.335, 26.831), when m is raised to 4. Because of the same unified conformational parameter, the phase diagram of Figure 3a is very similar to that of Figure 2b, except that the σ phase region of the former is shifted slightly toward the direction of increasing f. This verifies that the architecture asymmetry has a similar impact on the phase behaviors as the segment asymmetry.

Notice that the free energy difference per chain between the A15 and σ phases is at the order of 10^{-4} (see Figures S2), Comparisons of different free energy contributions reveal that the σ phase has more favorable stretching energy but higher interfacial energy than the A15 phase in the spherical phase region of high χN and large f (Figure S2). Therefore, A15 becomes stable after the σ phase when increasing f or χN. This prediction seems to be in agreement with the solution of the minimal surface area by Weaire and Phelan.[16] However, the packing mechanism of the spherical domains is different from that of the Kelvin problem because the latter has a restriction of equal volume but the former does not. In fact, the relative volumes of spherical domains in the A15 and σ phases are optimized in our calculations and become dissimilar. In addition, our SCFT results reveal that the average volume of spherical domains in the A15 phase is larger than that in the σ phase throughout the segregation region and the difference increases as the segregation degree increasing (see Figure S5). When we reduce the unit cell of A15 to achieve the same average volume of spherical domains as that of the σ phase, the interfacial energy of A15 becomes higher than that of the σ phase (see Figure S6). The phase sequence of the bcc, σ, and A15 phases with increasing χN is also consistent with that observed in the packing lattices of micelles formed by the amphiphilic superbranching liquid crystals.[1] In addition, our prediction that the σ phase has more preferential entropic energy than the A15 phase verifies the argument of the differential solid angle, which indicates that the σ phase with less close contacts has lower chain packing frustrations (or entropy penalty) of majority blocks than the A15 phase and therefore is more favored at higher temperatures.[1]

The stability region of the σ phase is identified by SCFT calculations in the phase region between the bcc and hexagonal phases in both the conformationally asymmetric AB diblock copolymers and AB_m miktoarm block copolymers, and it expands toward two directions of increasing and decreasing f as the conformational asymmetry increases. Our results elucidate that the architecture asymmetry has a similar effect on the phase behaviors as the segment asymmetry. However, the former factor can be more remarkably controlled and have a

dx.doi.org/10.1021/mz500445v | ACS Macro Lett. 2014, 3, 906−910

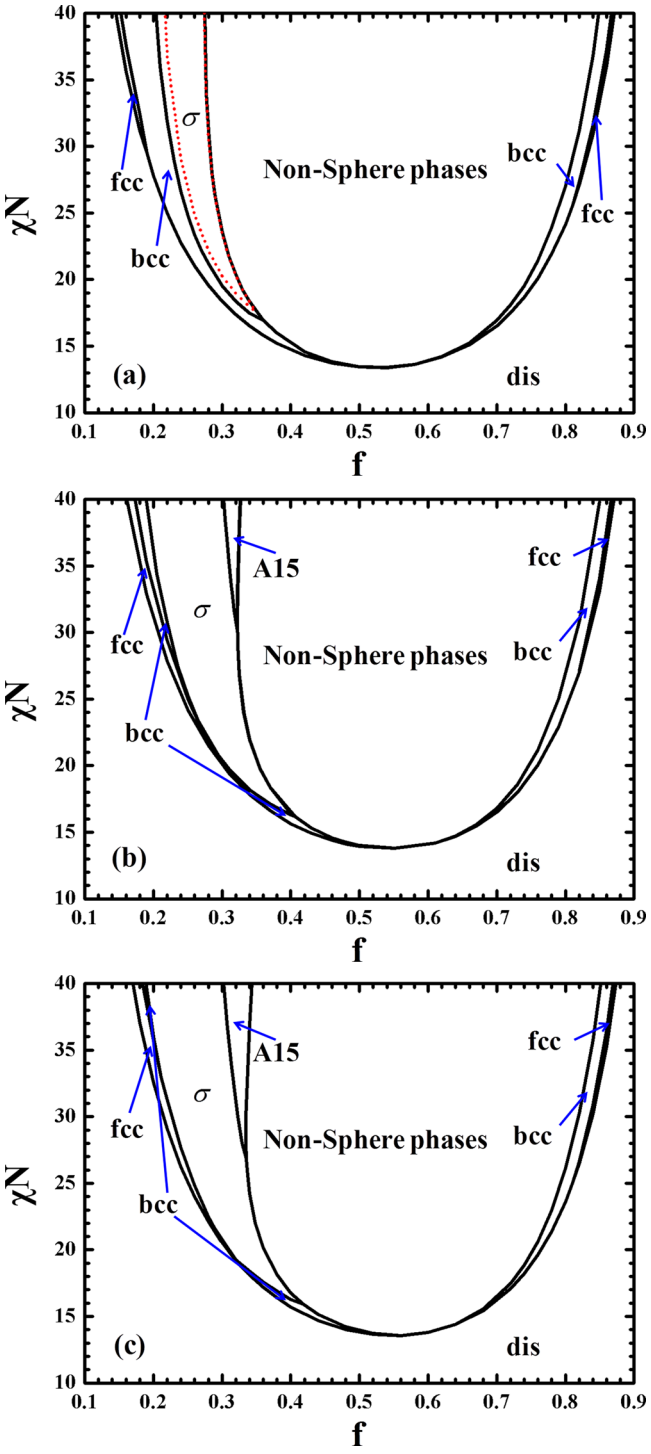

Figure 3. Phase diagrams of sphere phases for miktoarm AB_m block copolymers, with m = 2, 3, and 4 in (a), (b), and (c), respectively, from top to bottom. (a) For AB_2, the boundaries between the metastable phase A15 and the bcc and the hexagonal phases are plotted in red dashed lines.

much wider range to be tuned than the latter one. Only for the large architecture asymmetry, for example, m = 3 and 4, the A15 phase becomes stable in a noticeable phase region between the cylinder and σ phases. Therefore, branching or super-branching AB-type block copolymers can facilitate discovering the σ phase, or even the A15 phase in experiments. The conclusions on the relative stability between the different spherical phases also hold for the amphiphilic liquid crystal compounds because the intrinsic self-assembing mechasim is same. Moreover, these AB-type block copolymers with a significant stability region of the σ phase provide a useful platform to explore the quasicrystalline morphologies. In theory, the consideration of the σ phase significantly modifies the phase diagrams of the two conformationally asymmetric AB-type block copolymers, and thus supplements the structure bank of AB-type block copolymers.

■ ASSOCIATED CONTENT

Supporting Information

Further description and figures regarding the self-consistent field theory, the verification of accuracy dependence on the contour discretization, and comparisons of free energy and domain sizes between different phases. This material is available free of charge via the Internet at http://pubs.acs.org.

■ AUTHOR INFORMATION

Corresponding Author

*E-mail: weihuali@fudan.edu.cn.

Notes

The authors declare no competing financial interest.

■ ACKNOWLEDGMENTS

The authors thank M. Müller for helpful suggestion. This work was supported by the National Natural Science Foundation of China (NSFC; Grants Nos. 21322407 and 21174031).

■ REFERENCES

(1) Ungar, G.; Liu, Y. S.; Zeng, X. B.; Percec, V.; Cho, W. D. *Science* **2003**, *299*, 1208−1211.
(2) Zeng, X. B.; Ungar, G.; Liu, Y. S.; Percec, V.; Dulcey, A. E.; Hobbs, J. K. *Nature* **2004**, *428*, 157−160.
(3) Peterca, M.; Percec, V. *Science* **2010**, *330*, 333−334.
(4) McConnell, G. A.; Gast, A. P.; Huang, J. S.; Smith, S. D. *Phys. Rev. Lett.* **1993**, *71*, 2102−2105.
(5) McConnell, G. A.; Gast, A. P. *Phys. Rev. E* **1996**, *54*, 5447−5455.
(6) Balagurusamy, V.; Ungar, G.; Percec, V.; Johansson, G. *J. Am. Chem. Soc.* **1997**, *119*, 1539−1555.
(7) Percec, V.; Ahn, C. H.; Ungar, G.; Yeardley, D.; Möller, M.; Sheiko, S. S. *Nature* **1998**, *391*, 161−164.
(8) Cho, B. K.; Jain, A.; Gruner, S. M.; Wiesner, U. *Science* **2004**, *305*, 1598−1601.
(9) Sota, N.; Saijo, K.; Hasegawa, H.; Hashimoto, T. *Macromolecules* **2013**, *46*, 2298−2316.
(10) Ziherl, P.; Kamien, R. D. *Phys. Rev. Lett.* **2000**, *85*, 3528−3531.
(11) Huang, C. I.; Yang, L. F. *Macromolecules* **2010**, *43*, 9117−9125.
(12) Müller, M.; Sun, D. W. *Phys. Rev. Lett.* **2013**, *111*, 267801.
(13) Spencer, R. K. W.; Wickham, R. A. *Soft Matter* **2013**, *9*, 3373−3382.
(14) Xie, N.; Liu, M. J.; Deng, H. L.; Li, W. H.; Qiu, F.; Shi, A. C. *J. Am. Chem. Soc.* **2014**, *136*, 2974−2977.
(15) Thomson, W. *Philos. Mag.* **1887**, *24*, 503.
(16) Weaire, D.; Phelan, R. *Philos. Mag. Lett.* **1994**, *69*, 107−110.
(17) Bates, F. S.; Schulz, M.; Khandpur, A. K.; Förster, S.; Rosedale, J. H.; Almdal, K.; Mortensen, K. *Faraday Discuss.* **1994**, *98*, 7−18.
(18) Förster, S.; Khandpur, A. K.; Zhao, J.; Bates, F. S.; Hamley, I. W.; Ryan, A. J.; Bras, W. *Macromolecules* **1994**, *27*, 6922−6935.
(19) Khandpur, A. K.; Förster, S.; Bates, F. S.; Hamley, I. W.; Ryan, A. J.; Bras, W.; Almdal, K.; Mortensen, K. *Macromolecules* **1995**, *28*, 8796−8806.
(20) Matsen, M. W.; Schick, M. *Phys. Rev. Lett.* **1994**, *72*, 2660−2663.
(21) Drolet, F.; Fredrickson, G. H. *Phys. Rev. Lett.* **1999**, *83*, 4317−4320.

(22) Matsen, M. W. *J. Phys.: Condens. Matter* **2002**, *14*, R21−R47.
(23) Leibler, L. *Macromolecules* **1980**, *13*, 1602−1617.
(24) Matsen, M. W.; Bates, F. S. *Macromolecules* **1996**, *29*, 1091−1098.
(25) Matsen, M. W. *Eur. Phys. J. E* **2009**, *30*, 361−369.
(26) Bailey, T. S.; Hardy, C. M.; Epps, T. H., III; Bates, F. S. *Macromolecules* **2002**, *35*, 7007−7017.
(27) Tyler, C. A.; Morse, D. C. *Phys. Rev. Lett.* **2005**, *94*, 208302.
(28) Lee, S.; Bluemle, M. J.; Bates, F. S. *Science* **2010**, *330*, 349−353.
(29) Zhang, J. W.; Bates, F. S. *J. Am. Chem. Soc.* **2012**, *134*, 7636−7639.
(30) Matsen, M. W.; Bates, F. S. *J. Polym. Sci., Part B: Polym. Phys.* **1997**, *35*, 945−952.
(31) Milner, S. T. *Macromolecules* **1994**, *27*, 2333−2335.
(32) Olmsted, P. D.; Milner, S. T. *Macromolecules* **1998**, *31*, 4011−4022.
(33) Beyer, F. L.; Gido, S. P.; Velis, G.; Hadjichristidis, N.; Tan, N. B. *Macromolecules* **1999**, *32*, 6604−6607.
(34) Grason, G. M.; DiDonna, B. A.; Kamien, R. D. *Phys. Rev. Lett.* **2003**, *91*, 058304.
(35) Grason, G. M.; Kamien, R. D. *Macromolecules* **2004**, *37*, 7371−7380.
(36) Grason, G. M.; Kamien, R. D. *Phys. Rev. E* **2005**, *71*, 051801.
(37) Matsen, M. W. *Macromolecules* **2012**, *45*, 2161−2165.
(38) Rasmussen, K. O.; Kalosakas, G. *J. Polym. Sci., Part B: Polym. Phys.* **2002**, *40*, 1777−1783.
(39) Tzeremes, G.; Rasmussen, K. O.; Lookman, T.; Saxena, A. *Phys. Rev. E* **2002**, *65*, 041806.
(40) Lee, S.; Gillard, T. M.; Bates, F. S. *AIChE J.* **2013**, *59*, 3502−3513.